Acidity across the interface from the ocean surface to sea spray aerosol

Kyle J. Angle[a], Daniel R. Crocker[a], Rebecca M. C. Simpson[b], Kathryn J. Mayer[a], Lauren A. Garofalo[c], Alexia N. Moore[a], Stephanie L. Mora Garcia[a], Victor W. Or[a], Sudarshan Srinivasan[a], Mahum Farhan[b], Jon S. Sauer[a], Christopher Lee[b], Matson A. Pothier[c], Delphine K. Farmer[c], Todd R. Martz[b], Timothy H. Bertram[d], Christopher D. Cappa[e], Kimberly A. Prather[a,b], and Vicki H. Grassian[a,b,f,1]

[a]Department of Chemistry and Biochemistry, University of California San Diego, La Jolla, CA 92093; [b]Scripps Institution of Oceanography, University of California San Diego, La Jolla, CA 92093; [c]Department of Chemistry, Colorado State University, Fort Collins, CO 80523; [d]Department of Chemistry, University of Wisconsin–Madison, Madison, WI 53706; [e]Department of Civil and Environmental Engineering, University of California, Davis, CA 95616; and [f]Department of Nanoengineering, University of California San Diego, La Jolla, CA 92093

Aerosols impact climate, human health, and the chemistry of the atmosphere, and aerosol pH plays a major role in the physicochemical properties of the aerosol. However, there remains uncertainty as to whether aerosols are acidic, neutral, or basic. In this research, we show that the pH of freshly emitted (nascent) sea spray aerosols is significantly lower than that of sea water (approximately four pH units, with pH being a log scale value) and that smaller aerosol particles below 1 μm in diameter have pH values that are even lower. These measurements of nascent sea spray aerosol pH, performed in a unique ocean–atmosphere facility, provide convincing data to show that acidification occurs "across the interface" within minutes, when aerosols formed from ocean surface waters become airborne. We also show there is a correlation between aerosol acidity and dissolved carbon dioxide but no correlation with marine biology within the seawater. We discuss the mechanisms and contributing factors to this acidity and its implications on atmospheric chemistry.

aerosols | sea spray | acidity

Sea spray aerosol (SSA) profoundly impacts climate; however, aerosol–cloud interactions currently remain the largest source of uncertainty in climate modeling (1). With oceans covering ∼71% of Earth's surface, SSA significantly affects cloud properties and lifetime. Particle acidity has been shown to impact radiative forcing (2). Aerosol pH impacts the rates of multiphase reactions, including the oxidation of aqueous SO_2 by ozone and the formation of isoprene-derived secondary organic aerosol (3, 4). Furthermore, highly acidic aerosols can increase lung oxidative stress and adversely impact health (5, 6). Aerosol pH is difficult to measure, due to its dynamic nature and rapid response to changing environmental conditions such as relative humidity (RH). As such, there have been very few direct measurements of nascent SSA pH.

Atmospheric submicron SSA pH was first reported by Winkler (7), who collected ambient aerosols in water, diluted, measured pH and conductivity, and extrapolated to airborne aerosol pH assuming 90% RH. Depending on the extent of buffering, the resulting pH values fell between 1 and 3. Since this early study, there have been very few studies that directly measured SSA pH. This is likely due to the increasing use of thermodynamic models to calculate acidity from other measurements, as well as the difficulty of directly probing aerosol pH (8–10). However, models predict a wide range of aerosol pH values and can be highly sensitive to experimental uncertainties such as the error associated with ammonium measurements (11, 12). For example, reports applying model calculations to field data have reported SSA pH ranging from greater than 8 to below 0, depending on the location, meteorological conditions, and assumptions used in the model (13, 14). Furthermore, ambient aerosols are a mixture of nascent and aged particles. Thus, the acidity of nascent aerosols

is unknown, and direct measurements are needed. Specifically, size-resolved measurements of SSA pH are needed, since averaging pH in different particle size fractions can lead to pH variations of up to 3 pH units (6, 15).

It is often assumed that SSA has the same pH as seawater (∼8) (16, 17) and then can become acidified via mechanisms such as the uptake of acidic gases, water loss, and atmospheric aging reactions with sulfur dioxide (SO_2). Each of these processes proceeds on different timescales, with water loss occurring in seconds whereas some aging processes can take days (18, 19). Therefore, measuring the pH of nascent SSA (nSSA) is important since composition and pH vary with age. Here, we operationally define "nSSA" as SSA that has been airborne for less than 2 min. This investigation will give insight into the acidity of particles freshly emitted from the ocean.

Colorimetric pH strips have been successfully employed to sample aerosol pH, but results for ambient measurements have typically been semiquantitative at best. Ganor et al. (20) were limited to the resolution of 0.5 pH units provided by the pH paper manufacturer. Craig et al. (21) improved the method by using quantitative image analysis, although paper color for some field samples was incompatible with their analysis script. We optimized and thoroughly validated pH paper as a method to

Significance

Sea spray aerosol, produced through breaking waves, is one of the largest sources of environmental particles. Once in the atmosphere, sea spray aerosol influences cloud formation, serves as microenvironments for multiphase atmospheric chemical reactions, and impacts human health. All of these impacts are affected by aerosol acidity. Here we show that freshly emitted sea spray aerosol particles become highly acidic within minutes as they are transferred across the ocean–air interface. These results have important implications for atmospheric chemistry and climate, including aerosol/gas partitioning, heterogeneous reactions, and chemical speciation at the surface and within sea spray aerosol.

EARTH, ATMOSPHERIC, AND PLANETARY SCIENCES

determine real-world aerosol pH, and applied this technique to a sampling intensive called SeaSCAPE (Sea Spray Chemistry and Particle Evolution) where isolated SSAs were produced in a unique ocean–atmosphere facility. This study was carried out at the Hydraulics Laboratory at the Scripps Institution of Oceanography, using a sealed wave flume filled with coastal Pacific Ocean seawater obtained at 2 m of depth from the end of the Scripps pier. A paddle mechanically generates waves that break on a simulated beach within the flume, and it has been shown that this process produces a bubble size distribution similar to that of the real ocean (22). This facility allows for measurements of realistic nSSA in a clean and controlled environment devoid of other aerosols produced from pollution sources. Using a Micro-Orifice Uniform Deposit Impactor (MOUDI) and filters to aerodynamically distinguish aerosols in different size ranges, and impacting the aerosols onto pH strips, the size-resolved acidity of nSSA has been directly assessed.

Results

The size dependence of nSSA pH is shown in Fig. 1. These data are based on 106 measurements and show the general relationship of pH with aerosol aerodynamic diameter. The four leftmost bars are the results from MOUDI-separated nSSA collected at RH = 83 ± 5%, where particles from 0.1 microns to 1.0 microns in diameter (*SI Appendix*, Table S2) were found to have pH values between 1.5 and 2.6. The bar labeled "TSP" (total suspended particles) is the average result from filter-based measurements that collected all SSA sizes (see *SI Appendix*, Fig. S4 for a representative size distribution) at RH = 86 ± 6%. Although, strictly speaking, this is a measurement of the entire SSA ensemble pH, the results are far more reflective of supermicron pH than submicron pH, since, for this intensive, TSP was *ca.* 88% supermicron nSSA by mass. Therefore, we refer to TSP as supermicron. Note that the error bars in this figure represent 1 SD for each type of respective measurement pooled across the sampling intensive. For example, for TSP measurements, the error bar shows the SD calculated from the set of all TSP measurements. Even though these are not truly replicate measurements, since the flume water composition evolved over time, showing the error bars this way gives a visual representation of the range of values obtained over the course of the intensive.

For this study, extensive control experiments were performed to verify that the pH readings from the intensive were representative

of nSSA, rather than a result of experimental artifacts. Factors tested include the impact of variable salt concentration on pH paper color, the fading of pH paper color over time, the influence of gases on pH paper color, the mass loading needed for a pH reading, and the response of pH paper to various control aerosols. Notably, we found that even a 6 M change in NaCl concentration only changes the calculated submicron pH by, at most, 0.25 units (*SI Appendix*, Fig. S7), which is important considering that SSAs of different sizes can have substantially different salt fractions (23). Excluding this factor, the precision of the technique is ±0.17 pH units. For further details on these experiments, along with a full propagation of error, the reader is referred to *SI Appendix*.

Although variation of pH with size is small between the submicron size bins, the difference between supermicron and submicron pH is significant ($P = 7 \times 10^{-8}$, one-tailed t test). Since submicron and supermicron SSAs can have different salt concentrations, the t test was repeated assuming the maximum possible error (*SI Appendix, Uncertainty in pH Measurements and Propagation of Error*) by adding 0.7 pH units to every submicron value and subtracting 0.7 pH units from every supermicron value. The P value resulting from the t test is 0.001, indicating a statistically significant difference at 98%.

The pH of the sea surface microlayer (SSML, here operationally defined; see *SI Appendix, Materials and Methods*) was also measured throughout the sampling intensive. The average pH was 7.8 with an SD of 0.1 pH units. These results are generally consistent with past literature on SSML pH, with a slight decrease versus the subsurface sea water (SSW) pH of 8.1 ± 0.1, which was attributed to contact with atmospheric CO_2 (24). Calculating a paired t test for SSML pH and SSW pH averaged during the time of SSML collection (8:30 AM Pacific Time [PT] to 10:30 AM PT) gives a P value of 3×10^{-8}, showing the SSML is more acidic than the SSW. Given the air velocity in the wave flume and the distance from breaking waves to sampling ports in this study, and given the controls performed to account for paper color change after deposition, for these conditions, acidification of SSA appears to occur in less than 2 min. Thus, considering that the pH of the SSML is 7.8, substantial acidification occurs rapidly to increase the activity of H^+ in these aerosols by nearly six orders of magnitude in this short timescale.

A notable relationship is the correlation of SSA pH with SSW partial pressure of CO_2 (pCO$_2$) and pH (Fig. 2). This correlation is logical, since bulk water acidity is determined by the dissolved inorganic carbonate system, and, given that there were not significant changes in temperature or salinity, the similarity in R^2 values is unsurprising. However, the slope of 4.5 pH units in SSA pH per unit change in SSW pH indicates that the relationship must be controlled by acid–base systems other than carbonic acid. The correlation is likely indicative of how both SSA and SSW pHs change in response to an underlying factor. In addition, this relationship is only obtained using data points from the beginning of a phytoplankton bloom up until the flume was inoculated by the addition of separate, biologically dense water that had been obtained by the same method but kept out in sunlight to help induce biological activity. This inoculation turned the flume water greener and had a substantial impact on SSW chemical composition, including an SSW $[H^+]$ decrease of over 30% from the average preinoculation levels. When data points from this perturbation are included, the R^2 correlation coefficients of nSSA pH with pCO$_2$ and SSW pH become 0.03 and 0.04, respectively. Therefore, we tentatively hypothesize that nSSA pH is more predictable from CO_2 levels and ion concentrations when biological activity is minimal, while water with dense biological activity features more complicated pH relationships. Furthermore, as CO_2 levels increase in the atmosphere, these data show the potential for aerosols produced from ocean waters to be even more acidic.
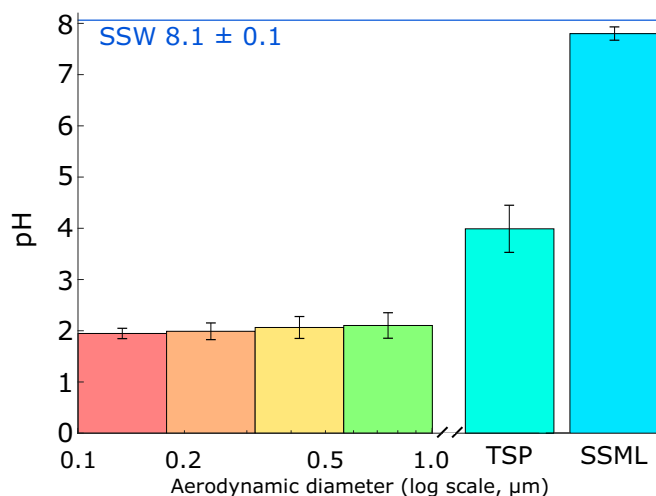

Fig. 1. Relationship between size and pH for SSA that is then compared to the SSML and bulk SSW. Error bars and the SSW uncertainty represent 1 SD for the respective measurements across the duration of the intensive. Note that TSP is predominantly a measure of supermicron SSA pH.
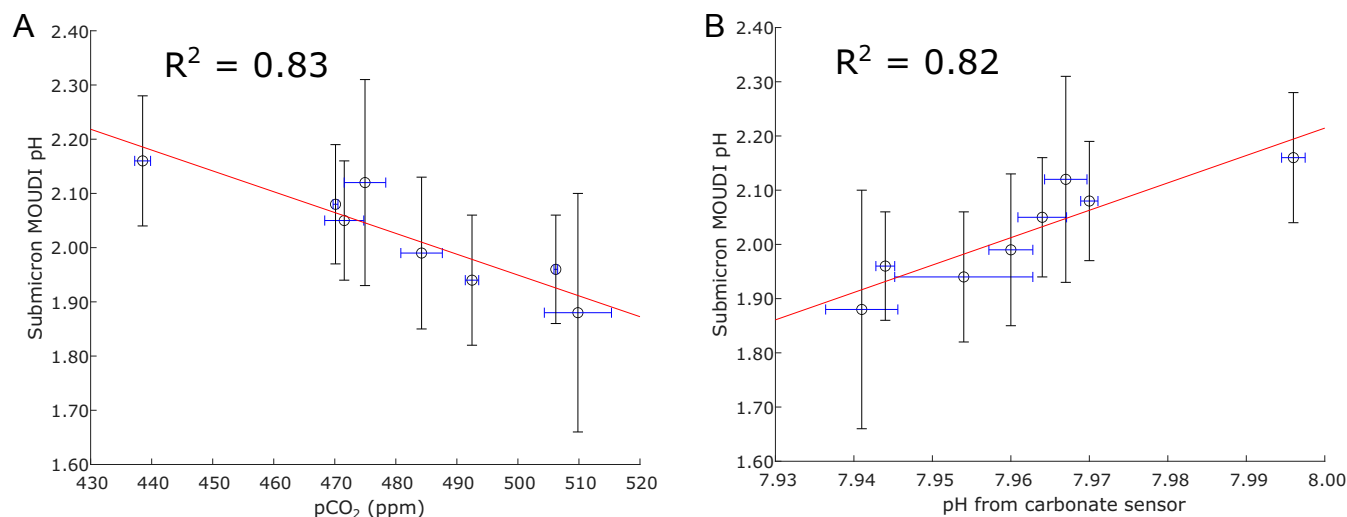
Fig. 2. (*A*) Inverse correlation between SSA pH and pCO_2; (*B*) correlation between SSA pH and seawater pH as calculated from pCO_2, dissolved inorganic carbon, temperature, and salinity. Data span from the addition of new seawater to the flume to perturbation by external inoculation. Horizontal error bars show 1 SD from minute averages during the corresponding MOUDI sampling time. Vertical error bars show 1 SD in nSSA pH calculated from different spots on the same pH strip.

At this time, we have not identified a single biological parameter that is predictive of nSSA pH. Further, while the microbial loop may impact aerosol pH, the impact is relatively small, as shown by the general stability of nSSA pH across substantial changes in phytoplankton and microbial activity as estimated by chlorophyll *a* concentrations (Fig. 3).

Discussion

Acidity Across the Interface. The results obtained here indicate that submicron aerosols obtain low pH rapidly after ejection from the ocean into the atmosphere. It has been suggested that this acidity in remote marine areas occurs in less than 15 min and perhaps even as fast as seconds (25–27). Here using a unique ocean wave facility, we can definitively conclude that nSSA is

Fig. 3. Time series of pH and chlorophyll *a* (Chl-a) measurements. Bulk seawater (SSW) pH, SSML pH, and nSSA pH from MOUDI stage 7 are plotted on the left-hand axis, and Chl-a concentration is plotted on the right-hand axis. The SSW and Chl-a traces reflect averages over every minute and 2 h, respectively, while symbols denote SSML and nSSA measurements.

acidic within the timescale of 2 min and that the acidity is volume (size) dependent.

The large change in acidity from supermicron to submicron SSAs has been previously discussed. Fridlind and Jacobson (28) calculated, for a model marine boundary layer, that submicrometer SSA comes to equilibrium with acidic gases within seconds, while hours are required for equilibrium with bases; for supermicrometer SSA, the opposite is true. The difference in acidity also follows from consideration of the surface area to volume (SA:V) ratios of these SSAs. The buffering capacity of a single SSA is proportional to its volume, while the rate of acid uptake (assuming a constant accommodation coefficient) is related to its surface area. Therefore, the buffering capacity is overwhelmed more rapidly for high SA:V, and, hence, submicron SSAs are more quickly acidified. The different mechanisms of formation also likely contribute to the acidity difference. Supermicron SSAs are mainly formed from jet drops, while submicron SSAs are mainly formed from both film and jet drops, with film drops having a greater enrichment of organic acids (29). It is possible that the submicron SSAs collected here were an external mixture of low pH (0 to 2) film drops and higher pH (2 to 4) jet drops, but future studies are needed to isolate these phenomena (30). We also emphasize that higher pH values would be observed in regions where dust or ammonia make a substantial contribution and neutralizes SSA acidity (31, 32).

It is worth noting that all submicron size bins had similar pH averages. Although Fig. 1 shows an apparent trend of slightly decreasing pH with diameter, the differences are not statistically significant at 95% confidence. Past investigators have found that, at pH = 2, the rates of acid uptake and HCl release are nearly equal for SSA, effectively buffering the aerosols at this pH (28). These results were obtained from a model of a remote marine boundary layer, removing the effects of further acidifying pollution and neutralizing mineral dust, and hence are similar to the conditions created here (13, 14, 25). It has also recently been shown by Zheng et al. (32) that the sulfate/bisulfate system buffers at pH of ~2 in aqueous solutions as well as aerosols, which could further contribute to buffering at this level.

Quantification of SSA pH is key to understanding various atmospheric chemical transformations. For example, hydrolysis of organic nitrates also occurs faster at lower pH (33). By
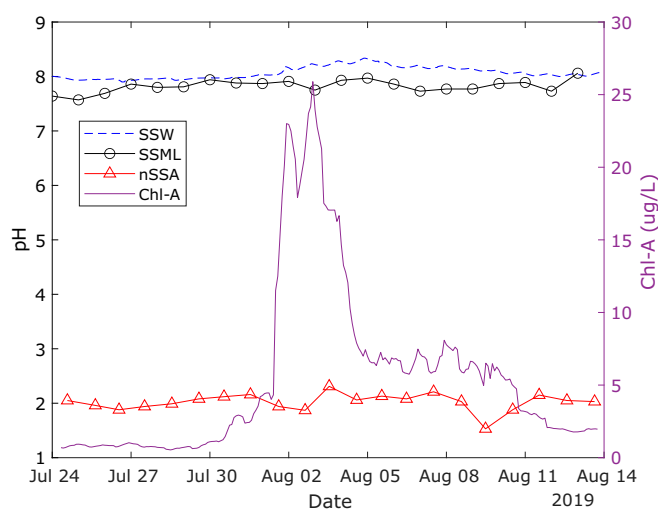
Angle et al.
Acidity across the interface from the ocean surface to sea spray aerosol

PNAS | 3 of 6
https://doi.org/10.1073/pnas.2018397118

contrast, the brown-carbon-forming reaction of glyoxal with amines is influenced by the proportion of unprotonated amines, leading to slower rates at lower pH (34). Many other examples exist, and it is clear that reactions that are important at the basic pH of seawater may be negligible at the highly acidic pH of submicron nSSA, and vice versa (12). For example, one particularly important atmospheric process with pH dependence is the oxidation of SO_2. This reaction produces sulfate and hence is important for predicting radiative forcing, and the fate of SO_2 depends strongly on the acidity of its environment (1). First, the effective Henry's law coefficient of SO_2 is over six orders of magnitude larger (in units of molars per atmosphere) at pH 8 vs. pH 2, indicating it will partition into submicron nSSA to a significantly lesser extent than previously thought (19). Combining Henry's law coefficient variability with kinetic parameters, Liang and Jacobson (35) calculated that, for pH = 8 SSA, 100 times more sulfate would be formed in the aqueous phase than the gas phase; for the same liquid water content at pH = 2, more sulfate would be formed in the gas phase instead. Second, the aqueous-phase oxidation of SO_2 has a highly complex pH dependence, proceeding by entirely different mechanisms for pH < 5 than for pH > 5 (36). Additionally, a rapid pathway of interfacial oxidation of SO_2 has been identified for aerosols with pH < 3.5 (37). Our data thus indicate this pathway is possible for submicron nSSA within minutes after its formation. Therefore, given the substantial contribution of SSA to atmospheric particulate mass and the pH dependence of the key SO_2 oxidation reaction, knowledge of the high acidity of nSSA is critical to accurately calculating the pathway and extent of sulfate formation and the subsequent impact on climate properties.

A compilation of pH ranges for marine aerosols is given in Table 1. These values span ranges similar to our findings; however, these other results are obtained from mixtures of nascent, atmospherically aged, and secondary marine aerosols. The low pH of aged SSA is often attributed to anthropogenic pollution, radicals, and oxidation of dimethyl sulfide to sulfur dioxide and sulfuric acid (13, 14, 16, 38), but those factors do not contribute to conditions here. Instead, the results shown here indicate acidification happens much more quickly. The prior studies, from field measurements, were not able to isolate nascent SSA, due to the nature of the measurements, whereas, here, we measured real-world samples in a controlled environment by bringing the "ocean into the lab" as described in Prather et al. (22). This allows for the determination that there are most likely several contributing mechanisms to the observed acidity of nSSA.

Factors Contributing to Low nSSA pH. RH is an important factor in assessing aerosol pH. Using readings from RH sensors before the MOUDI inlet and near the TSP filters, it was found that measured RH does not correlate ($R^2 = 0.01$) with submicron pH.

By contrast, the pH of supermicron SSA does correlate ($R^2 = 0.65$) with RH (SI Appendix, Fig. S6). Past calculations have indicated that submicron marine boundary layer aerosol pH only weakly corresponds to RH, where supermicron aerosol has a stronger dependence, which is in agreement with the findings here (28). This does not necessarily mean that RH plays no role in submicron aerosol pH but, rather, that there are additional factors impacting pH (39, 40). It is also worth noting that the RH range in question as measured at the MOUDI only spans 72 to 89%, so, at much lower RH, clearer trends of submicron SSA pH with water loss may be observed. The average RH values for the MOUDI, filters, and flume near particle generation were 83%, 86%, and 93%, respectively. Based on a typical growth factor curve for sodium chloride, the pH impact due to water loss moving from the site of generation to sampling was calculated. For the MOUDI and TSP filters, the pH of the measured nSSA before decreasing due to water loss would have been 0.3 and 0.2 units higher, respectively (41). Since RH data were only available for approximately half of the pH data points, and because this change is small, this correction was not applied to the data shown in Fig. 1, for consistency. However, for SSA over the real ocean, this factor may be more significant, as some of the lowest pH values (0 to −4) have been reported for conditions of low RH and high sulfate or organic concentrations (12, 13).

A second cause of acidic pH for nSSA to consider is the lowering of droplet pH by acidic gases. The headspace air used for SeaSCAPE was passed through chemical and particulate filters designed to scrub volatile organic compounds, nitrogen oxides, and particulates, including non-nSSA aerosols; however, they were unable to remove these species entirely (averaged over MOUDI collection times, the concentrations of NOx and O_3 were 0.9 ± 0.8 and 20 ± 7 parts per billion [ppb] by volume, respectively). It has been shown, from model calculations, that levels of HCl in the hundreds of parts per trillion range can acidify SSA pH by several units at 95% RH (28). Acidic gases at typical coastal concentrations could quickly bring nSSA to pH of ∼2 to 4, and the timescales associated with these processes are generally on the order of seconds to minutes for submicron SSA (19, 25, 28, 31, 42, 43). Supporting calculations outlined in SI Appendix show that 3 to 4 ppb total acidic gases would be sufficient to account for the pH values reported in this study. Due to logistical limitations, nitric acid and HCl concentrations were not measured, so the extent that acidic gases (or N_2O_5 converted to HNO_3) contributed to nSSA pH remains unknown. Additionally, controls were performed to rule out the changing of pH paper color due to direct interactions between the paper and the gases from the flume (SI Appendix, Discussion of Control Experiments for Aerosol pH Measurements).

Another source of acidity that may be particularly relevant to submicron aerosol pH is the dissociation of organic acids (23, 30). Surface-active species, particularly organics, are enriched in

Table 1. Compilation of selected submicron and supermicron marine aerosol pH values

Description	Submicrometer pH	Supermicrometer pH	Source
Aerosol leeching solutions from Hamburg, measured after dilution	1 to 3	4 to 8	(7)
Southern Ocean, calculated by an equilibrium model	0 to 2	2 to 5	(28)
Moderately polluted Bermuda, measured with minimal dilution	−1.1 to 3.2	1.2 to ≥5.6	(14)
Hawaiian marine boundary layer, inferred from phase partitioning	2.6 to 5.3	4.5 to 5.4	(27)
Hawaiian after volcanic plume, measurement-constrained ISORROPIA	−0.8 to 3.0	N/A	(54)
Eastern Mediterranean, calculated from measurement of LWC	−0.2 to 1.1	∼7*	(13)
Various Southern Ocean locations, PM$_{2.5}$, calculated by ISORROPIA	N/A	0.5 to 4.1	(55)
Nascent SSA from controlled ocean-atmosphere facility using Pacific Ocean waters, colorimetric measurements	1.5 to 2.6	3.5 to 4.7	This work

*This is a measure of PM$_{10}$; reported as less quantitative than the corresponding submicrometer measurement. LWC, liquid water content; N/A, not applicable.

the aerosol phase, predominately in smaller particles (44). For a 200-nm-diameter SSA with a surface layer of palmitic acid with a mean molecular area of 22 Å^2, only 4.4% acid dissociation is required to lower pH from 8 to 2. Although weak fatty acids typically dissociate only ~1% on their own, high concentrations of NaCl can shift acid pK_a values and increase dissociation as Na$^+$ ions compete with H$^+$ for binding (45, 46). Since SSA often have higher concentrations of salt than the SSW and SSML, this cation-assisted dissociation becomes more important as the molecules are transferred across the ocean–air interface (47). Further, as water is lost after the SSAs are emitted from the ocean, the resulting simultaneous concentration of organic acids and NaCl could enhance this phenomenon and lead to deprotonation that significantly impacts SSA pH. Given that it is known that surface-active species are enriched at and across the air/water interface (44), it is reasonable that this enrichment impacts the change in pH across this interface upon aerosol formation (45).

Finally, as a point of comparison, we applied the Extended Aerosol Inorganics Model (E-AIM) to data from a High-Resolution Aerosol Mass Spectrometer (HR-AMS) to estimate aerosol pH (48). We used Inorganic Model II, which uses concentrations of H$^+$, NH$_4^+$, SO$_4^{2-}$, NO$_3^-$, and H$_2$O as inputs (see *SI Appendix*, Table S3 for values) (39, 49, 50). The observed NH$_4^+$ was low and near the limit of detection, and the AMS is unable to quantitatively measure refractory components (i.e., NaCl). To this end, we performed two sets of calculations. First, we used the observed values, which gave calculated aerosol pH of -0.62 ± 0.07. Separately, we enhanced NH$_4^+$ to neutralize SO$_4^{2-}$ (to act as a proxy for the unobserved cations; on average, this increased the NH$_4^+$ input by a factor of 2.1), which gave calculated aerosol pH of -0.1 ± 0.3. These pH values should not be taken as the quantitative equilibrium acidity of these particles: Using E-AIM without gas-phase inputs can yield highly variable results (8), and we acknowledge that the enhancing of NH$_4^+$ to approximate unmeasured cations is imperfect. Additionally, these pH values may be low, because all sulfate is assumed to be inorganic, when a fraction may instead originate from organosulfur compounds (51). Even so, these results emphasize that the AMS observations and associated calculations do support the major conclusion of this work that submicron nSSAs are highly acidic.

Combining the sudden drop in pH with the substantial increase in concentration that these aerosols undergo due to water loss, nSSAs could serve as microreactors for chemical reactions that do not occur in SSW. Further, considering the lifespan of submicron SSA is on the order of days, these aerosols are only alkaline for a nearly negligible portion of their existence immediately after ejection from the ocean, and subsequently remain highly acidic until further processing such as coalescence or deposition (52). Therefore, models of submicron SSA should treat nSSA as acidic, rather than pH of ~8, since the former is a far better representation of the chemical environment inside these aerosols for the vast majority of their atmospheric lifetimes. This, in turn, will impact the chemical composition both inside the aerosols and in the atmosphere, as particle pH influences aerosol/gas partitioning and the fate of pollutants such as SO$_2$ (37).

Overall, the pH of isolated nSSA has been directly measured under controlled conditions. The aerosol is highly acidic, showing that even freshly emitted SSA has a substantially lower pH than the bulk seawater. Additionally, these findings show that size-resolved submicron aerosol pH can be measured within hours to help capture variations in pH as other conditions evolve. From seawater to the SSML to supermicron and submicron aerosol, a trend with pH and volume becomes clear. The increasing acidity with decreasing volume may be due to a variety of phenomena, such as enrichment of acidic organic species. Regardless of the cause, this abrupt and clear decrease in pH across the ocean–air interface has important implications for various processes, including acid-catalyzed chemical reactions, sulfur(IV) oxidation, and surface partitioning of gases in the aerosol. Most importantly, these results show nSSA is acidified within minutes of aerosol formation without interaction with high levels of pollution that are typically considered to be important for aerosol acidification. These measurements of nSSA acidity inform models calculating the rate of critical atmospheric chemical transformations.

Materials and Methods

A full description of materials and methods is given in *SI Appendix*. For size-resolved measurements, pH strips (Hydrion) were attached to aluminum foil discs with double-sided tape, then affixed to 110-R MOUDI (MSP) pucks using the associated metal rings. The MOUDI was connected to the wave channel (Hydraulics Laboratory) and operated with rotation at 30 L per min. The wave channel generated nSSA (for the size distribution, see *SI Appendix*, Fig. S4). Collection of these SSAs into the MOUDI typically proceeded for 1 h to 2 h. After collection, the MOUDI was disassembled, and photographs of the pH strips were taken immediately. Images were processed using a custom MATLAB code (see *Data Availability*). For TSP measurements, the procedure was the same, except filter holders were used in place of a MOUDI, a flow rate of 5.5 L per min was used, and collection times typically ranged from 30 min to 60 min. SSML pH was measured by both pH paper and a pH probe using samples obtained by dipping a glass plate in the wave channel. A suite of sensors was used to measure SSW properties including temperature, salinity, and chlorophyll a (SeaBird Scientific SBE16 with Eco-Triplet BBFL2); pH (Honeywell Durafet); dissolved oxygen (Aanderaa Data Instruments 3835 Optode); and pCO$_2$ and total dissolved inorganic carbon ("Burke-o-lator" custom IR analyzer). An HR time-of-flight AMS provided bulk speciated aerosol mass concentrations (48). The AMS was operated in V ion path (m/Δm = 2,500) in mass spectra and particle time-of-flight modes.

1. O. Boucher et al, "Clouds and aerosols" in Climate Change 2013: The Physical Science Basis. Contribution of Working Group I to the Fifth Assessment Report of the Intergovernmental Panel on Climate Change (Intergovernmental Panel on Climate Change, 2013), T. Stocker et al, Eds. (Cambridge University Press, Cambridge, U.K.), pp. 571–657.
2. J. Duan et al., Particle liquid water content and aerosol acidity acting as indicators of aerosol activation changes in cloud condensation nuclei (CCN) during pollution eruption in Guangzhou of South China. Aerosol Air Qual. Res. 19, 2662–2670 (2019).
3. B. Alexander et al., Sulfate formation in sea-salt aerosols: Constraints from oxygen isotopes. J. Geophys. Res. Atmos. 110, 1–12 (2005).
4. Y. Zhang et al., Joint impacts of acidity and viscosity on the formation of secondary organic aerosol from isoprene epoxydiols (IEPOX) in phase separated particles. ACS Earth Space Chem. 3, 2646–2658 (2019).
5. M. A. Freedman, E. E. Ott, K. E. Marak, Role of pH in aerosol processes and measurement challenges. J. Phys. Chem. A 123, 1275–1284 (2019).
6. T. Fang et al., Highly acidic ambient particles, soluble metals, and oxidative potential: A link between sulfate and aerosol toxicity. Environ. Sci. Technol. 51, 2611–2620 (2017).
7. P. Winkler, "Relations between aerosol acidity and ion balance" in Chemistry of Multiphase Atmospheric Systems, W. Jaeschke, Ed. (Springer, Berlin, Germany, 1986), pp. 269–298.
8. C. J. Hennigan, J. Izumi, A. P. Sullivan, R. J. Weber, A. Nenes, A critical evaluation of proxy methods used to estimate the acidity of atmospheric particles. Atmos. Chem. Phys. 15, 2775–2790 (2015).
9. E. M. Coddens, K. J. Angle, V. H. Grassian, Titration of aerosol pH through droplet coalescence. J. Phys. Chem. Lett. 10, 4476–4483 (2019).

Angle et al.
Acidity across the interface from the ocean surface to sea spray aerosol

10. F. W. Lipfert, S. C. Morris, R. E. Wyzga, Acid aerosols: The next criteria air pollutant? *Environ. Sci. Technol.* **23**, 1316–1322 (1989).

11. H. Guo, A. Nenes, R. J. Weber, The underappreciated role of nonvolatile cations in aerosol ammonium-sulfate molar ratios. *Atmos. Chem. Phys.* **18**, 17307–17323 (2018).

12. H. O. T. Pye *et al.*, The acidity of atmospheric particles and clouds. *Atmos. Chem. Phys.* **20**, 4809–4888 (2020).

13. A. Bougiatioti *et al.*, Particle water and pH in the eastern Mediterranean: Source variability and implications for nutrient availability. *Atmos. Chem. Phys.* **16**, 4579–4591 (2016).

14. W. C. Keene, A. A. P. Pszenny, J. R. Maben, R. Sander, Variation of marine aerosol acidity with particle size. *Geophys. Res. Lett.* **29**, 1101 (2002).

15. J. Ludwig, O. Klemm, Acidity of size-fractionated aerosol particles. *Water Air Soil Pollut.* **49**, 35–50 (1990).

16. D. Katoshevski, A. Nenes, J. H. Seinfeld, A study of processes that govern the main-tenance of aerosols in the marine boundary layer. *J. Aerosol Sci.* **30**, 503–532 (1999).

17. K. A. Carter-Fenk, H. C. Allen, Collapse mechanisms of nascent and aged sea spray aerosol proxy films. *Atmosphere (Basel)* **9**, 1–16 (2018).

18. G. Rovelli, R. E. H. Miles, J. P. Reid, S. L. Clegg, Accurate measurements of aerosol hygroscopic growth over a wide range in relative humidity. *J. Phys. Chem. A* **120**, 4376–4388 (2016).

19. J. H. Seinfeld, S. N. Pandis, "Chemistry of the atmospheric aqueous phase" in *At-mospheric Chemistry and Physics: From Air Pollution to Climate Change* (John Wiley, ed. 3, 2016), pp. 265–324.

20. E. Ganor, Z. Levin, D. Pardess, Determining the acidity and chemical composition of fog, haze and cloud droplets in Israel. *Atmos. Environ., A Gen. Topics* **27**, 1821–1832 (1993).

21. R. L. Craig *et al.*, Direct determination of aerosol pH: Size-resolved measurements of submicrometer and supermicrometer aqueous particles. *Anal. Chem.* **90**, 11232–11239 (2018).

22. K. A. Prather *et al.*, Bringing the ocean into the laboratory to probe the chemical complexity of sea spray aerosol. *Proc. Natl. Acad. Sci. U.S.A.* **110**, 7550–7555 (2013).

23. T. H. Bertram, R. E. Cochran, V. H. Grassian, E. A. Stone, Sea spray aerosol chemical composition: Elemental and molecular mimics for laboratory studies of heteroge-neous and multiphase reactions. *Chem. Soc. Rev.* **47**, 2374–2400 (2018).

24. Z. Zhang, W. Cai, L. Liu, C. Liu, F. Chen, Direct determination of thickness of sea surface microlayer using a pH microelectrode at original location. *Sci. China B Chem.* **46**, 339–351 (2003).

25. W. C. Keene, A. A. P. Pszenny, Aerosol pH in the marine boundary layer: A review and model evaluation. *J. Aerosol Sci.* **29**, 339–356 (1998).

26. M. E. Salter *et al.*, Calcium enrichment in sea spray aerosol particles. *Geophys. Res. Lett.* **43**, 8277–8285 (2016).

27. A. A. P. Pszenny *et al.*, Halogen cycling and aerosol pH in the Hawaiian marine boundary layer. *Atmos. Chem. Phys.* **4**, 147–168 (2004).

28. A. M. Fridlind, M. Z. Jacobson, A study of gas-aerosol equilibrium and aerosol pH in the remote marine boundary layer during the First Aerosol Characterization Experi-ment (ACE 1). *J. Geophys. Res. Atmos.* **105**, 17325–17340 (2000).

29. R. E. Cochran *et al.*, Molecular diversity of sea spray aerosol particles: Impact of ocean biology on particle composition and hygroscopicity. *Chem* **2**, 655–667 (2017).

30. X. Wang *et al.*, The role of jet and film drops in controlling the mixing state of submicron sea spray aerosol particles. *Proc. Natl. Acad. Sci. U.S.A.* **114**, 6978–6983 (2017).

31. G. Shi *et al.*, pH of aerosols in a polluted atmosphere: Source contributions to highly acidic aerosol. *Environ. Sci. Technol.* **51**, 4289–4296 (2017).

32. G. Zheng *et al.*, Multiphase buffer theory explains contrasts in atmospheric aerosol acidity. *Science* **369**, 1374–1377 (2020).

33. J. D. Rindelaub *et al.*, The acid-catalyzed hydrolysis of an α-pinene-derived organic nitrate: Kinetics, products, reaction mechanisms, and atmospheric impact. *Atmos. Chem. Phys.* **16**, 15425–15432 (2016).

34. N. Sedehi, H. Takano, V. A. Blasic, K. A. Sullivan, D. O. De Haan, Temperature- and pH-dependent aqueous-phase kinetics of the reactions of glyoxal and methylglyoxal with atmospheric amines and ammonium sulfate. *Atmos. Environ.* **77**, 656–663 (2013).

35. J. Liang, M. Z. Jacobson, A study of sulfur dioxide oxidation pathways over a range of liquid water contents, pH values, and temperatures. *J. Geophys. Res.* **104**, 749–762 (1999).

36. C. Brandt, R. van Eldik, Transition metal-catalyzed oxidation of sulfur(IV) oxides: Atmospheric-relevant processes and mechanisms. *Chem. Rev.* **95**, 119–190 (1995).

37. H. M. Hung, M. N. Hsu, M. R. Hoffmann, Quantification of SO_2 oxidation on interfacial surfaces of acidic micro-droplets: Implication for ambient sulfate formation. *Environ. Sci. Technol.* **52**, 9079–9086 (2018).

38. S. Wang, M. Maltrud, S. Elliott, P. Cameron-Smith, A. Jonko, Influence of dimethyl sulfide on the carbon cycle and biological production. *Biogeochemistry* **138**, 49–68 (2018).

39. S. L. Clegg, P. Brimblecombe, A. S. Wexler, Thermodynamic model of the system $H^+–NH_4^+–SO_4^{2-}–NO_3^−–H_2O$ at tropospheric temperatures. *J. Phys. Chem. A* **102**, 2137–2154 (1998).

40. R. Von Glasow, R. Sander, Variation of sea salt aerosol pH with relative humidity. *Geophys. Res. Lett.* **28**, 247–250 (2001).

41. T. Pinterich, S. R. Spielman, Y. Wang, S. V. Hering, J. Wang, A humidity-controlled fast integrated mobility spectrometer (HFIMS) for rapid measurements of particle hy-groscopic growth. *Atmos. Meas. Tech.* **10**, 4915–4925 (2017).

42. E. Harris *et al.*, Sulfur isotope fractionation during heterogeneous oxidation of SO_2 on mineral dust. *Atmos. Chem. Phys.* **12**, 4867–4884 (2012).

43. W. Hoppel *et al.*, Sulfur dioxide uptake and oxidation in sea-salt aerosol. *J. Geophys. Res. Atmos.* **106**, 27575–27585 (2001).

44. R. E. Cochran, T. Jayarathne, E. A. Stone, V. H. Grassian, Selectivity across the inter-face: A test of surface activity in the composition of organic-enriched aerosols from bubble bursting. *J. Phys. Chem. Lett.* **7**, 1692–1696 (2016).

45. T. Zhang *et al.*, Effect of pH and salt on surface pK_a of phosphatidic acid monolayers. *Langmuir* **34**, 530–539 (2018).

46. T. Zhang, M. G. Cathcart, A. S. Vidalis, H. C. Allen, Cation effects on phosphatidic acid monolayers at various pH conditions. *Chem. Phys. Lipids* **200**, 24–31 (2016).

47. J. Turšič, I. Grgić, B. Podkrajšek, Influence of ionic strength on aqueous oxidation of SO_2 catalyzed by manganese. *Atmos. Environ.* **37**, 2589–2595 (2003).

48. P. F. DeCarlo *et al.*, Field-deployable, high-resolution, time-of-flight aerosol mass spectrometer. *Anal. Chem.* **78**, 8281–8289 (2006).

49. S. L. Clegg, K. S. Pitzer, P. Brimblecombe, Thermodynamics of multicomponent, mis-cible, ionic solutions. 2. Mixtures including unsymmetrical electrolytes. *J. Phys. Chem.* **96**, 9470–9479 (1992).

50. A. S. Wexler, S. L. Clegg, Atmospheric aerosol models for systems including the ions H^+, NH_4^+, Na^+, SO_4^{2-}, NO_3^-, Cl^-, Br^-, and H_2O. *J. Geophys. Res. Atmos.* **107**, 4207 (2002).

51. Y. Chen *et al.*, Response of the aerodyne aerosol mass spectrometer to inorganic sulfates and organosulfur compounds: Applications in field and laboratory mea-surements. *Environ. Sci. Technol.* **53**, 5176–5186 (2019).

52. G. De Leeuw *et al.*, Production flux of sea spray aerosol. *Rev. Geophys.* **49**, RG2001 (2011).

53. K. J. Angle *et al*, Data from "Acidity across the interface: From the ocean surface to sea spray aerosol." Center for Aerosol Impacts on Chemistry of the Environment (CAICE) UC San Diego Library Digital Collections. https://doi.org/10.6075/J028065J. Deposited 1 October 2020.

54. J. H. Kroll *et al.*; TREX XII; TREX XI, Atmospheric evolution of sulfur emissions from Kīlauea: Real-time measurements of oxidation, dilution, and neutralization within a volcanic plume. *Environ. Sci. Technol.* **49**, 4129–4137 (2015).

55. M. Dall'Osto *et al.*, Simultaneous detection of alkylamines in the surface ocean and atmosphere of the antarctic sympagic environment. *ACS Earth Space Chem.* **3**, 854–862 (2019).

6 of 6 | **PNAS**
https://doi.org/10.1073/pnas.2018397118

Angle et al.
Acidity across the interface from the ocean surface to sea spray aerosol